Light emission from randomly rough tunnel junctions

P. D. Sparks and J. E. Rutledge
Physics Department, University of California, Irvine, California 92717
(Received 12 May 1989)

Randomly rough tunnel junctions are known to emit visible light when biased at voltages that correspond to optical frequencies. It has been established that surface-plasmon polaritons (SPP's) mediate the light output, but experiments have been interpreted to identify different SPP modes as the most important to the process. Different points of view on how the SPP modes are excited have also persisted. A series of measurements on a large number of aluminum-gold junctions that identifies the so-called slow mode as the dominant mode is reported here. This conclusion is independent of the details of theories of the light-emission process. We have also calculated the electric fields and the resulting optical spectra from biased junctions. The numerical results confirm the slow mode as the dominant mode and when compared with our data imply that inelastic tunneling current fluctuations confined to the tunneling barrier are responsible for the emitted light.

I. INTRODUCTION

In 1976 Lambe and McCarthy reported the emission of light from metal-oxide–metal tunnel junctions.[1] They also identified a particular surface-plasmon-polariton (SPP) mode as the source of the light and presented evidence that the mode was driven by inelastic tunneling current fluctuations. Since then a great deal of work has been done to further clarify the emission mechanism and to try to determine how much light these devices might produce. Many ingenious experiments have been performed, and quantitative theories have been developed to explain them.[2] As a consequence of these activities, alternative candidates for both the dominant mode and for the driving mechanism have emerged.

A large number of emission mechanisms must be considered. A tunnel junction supports three modes in the visible. A junction consists of a thick insulating substrate covered with a metal film a few tens of nanometers thick. This film is allowed to oxidize to a thickness of 3 nm or so and is then covered with a second metal film of comparable thickness to the first. Counting the medium above the second metal, a junction consists of five media separated by four interfaces. If this structure is driven by impressing a fictitious current density in it, the modes appear. Consider a current density given by $\mathbf{J}_0\delta(z-z_0)\times\exp[i(k_\parallel x-\omega t)]$, where $\mathbf{J}_0$ is independent of position, z is the coordinate normal to the plane of the junction, z_0 may lie within or above or below the junction, $k_\parallel$ is a wave vector lying in the plane of the junction, and ω is an optical frequency. Impressing this current density will induce electric fields of the form $\mathbf{E}(z)\exp[i(k_\parallel x-\omega t)]$ throughout all five media. Although the details will depend on the polarization and z_0, a contour plot of $|\mathbf{E}(z)|^2$ on the $k_\parallel$-ω plane will, in general, show three ridges of relative maxima in the optical frequency range. These ridges are the modes.

The locations of the modes for a 20-nm au, 3-nm aluminum oxide, 20-nm Al junction are shown in Fig. 1. The heights of the ridges depend on z. The ridge just to the right of the free-photon dispersion curve is highest at the top surface of the second metal film, and it dominates the other two modes there. This paper discusses experiments on junctions with aluminum for the first metal and gold for the second. We will call this mode the Au fast mode. The highest fields at the Al-substrate interface lie along the ridge that lies just to the right of the dispersion curve of photons in the glass substrate. We will call this mode the Al fast mode. The third ridge lies along a curve of much slower phase velocity than the other two and is called the slow mode. Its maximum field strength is located in the oxide barrier between the metal films, where it dominates the field strength of the other two modes.

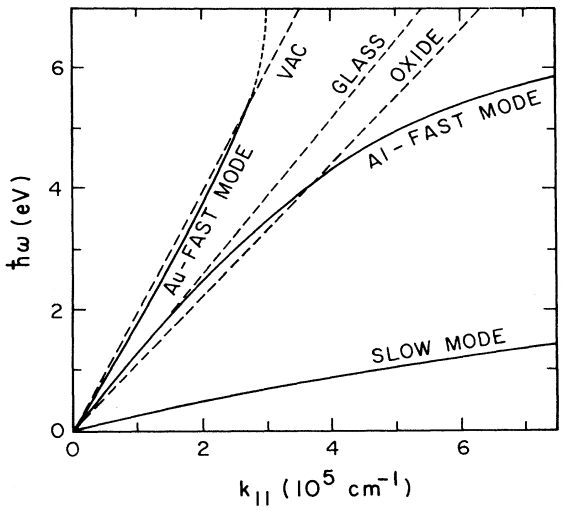

FIG. 1. Positions of the modes in the $k_\parallel$-ω plane. The modes are ridges of relative maxima in the E-field intensity for junctions driven harmonically. These results for a 20-nm Au, 2-nm oxide, 20-nm Al junction are from Ref. 6.

Under suitable conditions, energy from any of these modes can be scattered into visible light above or below the junction.

To completely characterize the emission process, the mechanism that drives the modes must be identified as well. Several possibilities present themselves here also. The original mechanism suggested was inelastic tunneling current fluctuations. These result from the overlap of the wave functions of electrons of different energies on opposite sides of the barrier. The overlap region is restricted to the oxide barrier. It was suggested that this mechanism must be modified by extending the current fluctuations into the metal films in order to account for the intensity observed from real junctions.[3] There is evidence that suggests that electrons that tunnel elastically from one film to the other can excite at least the top metal-film fast mode. This is called the hot-electron mechanism and is a third possibility for the drive term.[4] So, even if attention is restricted to the modes and drive mechanisms just discussed, there is a large number of possible combinations to sort out before the emission mechanism can be determined.

Perhaps the most significant reason that the emission mechanism has defied identification for so long is that there are junction parameters that are hard to control, or even to measure, that are critically important in the light-emission process. The first of these is the random roughness that is present on every interface. Except for the Au fast mode leaking into the substrate, none of the modes can radiate into the medium above or below the metal films unless it scatters off some deviation from flatness. The modes are forbidden to radiate directly because their wave vectors exceed the wave vector of photons anywhere outside the metal. Anything that breaks the two-dimensional translational symmetry of the structure will suffice to allow the modes to radiate, including the random roughness that all real junctions have whether or not they are intentionally roughened. Even in experiments that have included some other means for allowing a particular mode to radiate, such as experiments on gratings or prisms, the random roughness provides another emission channel that can complicate the interpretation of the experimental results. The most harmful aspect of the roughness is that it does not reproduce exactly on otherwise identical samples. There is a similar problem with the dielectric functions of the metal films. It is known at least for Au that the dielectric function of evaporated films depends on details of the deposition conditions.[5]

Finally, in the course of the work reported here, we have noticed that at least for Al-Au junctions run at room temperature in air, the behavior of the tunneling barrier depends on how long and at what bias voltage the junction has been run. The combination of these three poorly reproducible effects produces variations in the spectra of even nominally identical samples that mask the systematic behavior one searches for to identify the emission mechanism. Thus, data from a small number of samples can seem to support almost any mechanism.

This paper presents the results of a systematic study of 66 Au-oxide–Al light-emitting tunnel junctions. We have studied junctions with both film thicknesses ranging between about 20 and 130 nm for either film. All of the data presented here have been reproduced in several samples of the same kind, ensuring that none of our conclusions are based on the behavior of a single junction. Independently of the details of any model or calculation, except for the general picture of the modes presented above, the data show that the light emitted from either side by randomly rough Au-Al junctions is scattered almost entirely from the slow mode. We have also calculated the emission expected from a Au-oxide–Al junction. Our model is incomplete because we can only calculate the light emitted perpendicularly to either surface. Nevertheless, the numerical results support the conclusion that the slow mode dominates the emission process. They also suggest that the scattering of this mode is dominated by roughness at the edges of the oxide barrier[6] and that inelastic tunneling fluctuations confined to the oxide barrier are responsible for driving the mode. We have reached the same conclusions Lambe and McCarthy did.

The rest of the paper presents the data and arguments that lead to these conclusions. Section II gives some of the experimental details. Section III presents the results of our measurements. First, we will describe an aging process that plagues Au-oxide–Al samples run at room temperature. This process and sample-to-sample deviations in the roughness and dielectric function must be appreciated before the measurements can be interpreted. Then we will present the data that lead to the identification of the slow mode as the dominant mode. In Sec. IV we will describe our calculation and present calculated $|\mathbf{E}(z)|^2$ contours and emission spectra that support our experimental conclusion. We will also show that our model suggests that tunneling current fluctuations confined to the oxide barrier are the driving mechanism. Section V is a discussion of the relationship of these results to earlier work.

II. EXPERIMENT

The tunnel junctions were deposited by thermal evaporation onto microscope cover slips which had been cleaned with detergent and water, boiled in 3:1 H_2O_2:NH_3OH solution, and degreased in methanol, trichloroethylene, and acetone. The films were deposited in a standard liquid-nitrogen-trapped diffusion-pumped vacuum system at pressures of $(3-5)\times10^{-6}$ Torr. All of the junctions we will report on here were Au-Al junctions with aluminum oxide forming the tunneling barrier. The Al films were deposited on the cleaned cover slips from tungsten baskets at a rate of 0.5 nm/s. The oxide barrier was grown either by heating in air at 200 °C for 5 min or in a plasma discharge in a 200-mTorr atmosphere for 5 min. There was no difference in the behavior of the junctions made by the different oxidation processes. The junctions were completed by masking the edges of the oxidized Al film with optical cement and evaporating the Au film at a rate of 0.1 nm/s from an alumina-coated tungsten filament.

The junctions were formed by overlapping the ends of

two aligned, parallel films 0.2 cm wide. The overlap region was 0.1 cm long. This geometry minimizes the voltage smearing due to the finite resistances of the two films.[7] The careful cleaning of the substrates and the masking of the edges of the aluminum film and slow Au deposition seemed to increase the lifetime of the junction. We could usually run a junction for about 5 h and some ran for about a day. All of the spectra we took were taken with the Au film biased positively because reversing the polarity rapidly burned out our samples.

Almost all of the data presented here consist of spectra taken normal to either the gold or the aluminum film. The collection optics accepted all the light in a cone of half-angle 18° around the optical axis. We found that, unless we used achromatic doublets exclusively in the collection system, the measured spectra from the extended sources our junctions presented were extremely sensitive to small differences in the optical alignment. The spectra of the light emitted by the junction were measured with a SPEX 1400-11 grating spectrometer, a Hamamatsu R943-02 photomultiplier, and photon-counting electronics. The resolution in wavelength was 3 nm. The raw data of count rate per unit wavelength *versus* wavelength were corrected for the detection efficiency of the spectrometer and photomultiplier using measured spectra of an unpolarized tungsten-filament standard lamp through a junction-sized aperture focussed on the entrance slit of the spectrometer by the collection optics used with the junctions. Finally, the data were numerically converted to (counts/s)/(unit energy/A) *versus* photon energy. We did not measure the absolute detection efficiency of the system and so cannot comment on the absolute quantum efficiency of the junctions. But any two of our measured spectra can be directly compared to establish their relative efficiency.

Our tunnel junctions were voltage biased by an active circuit and the bias current was continuously monitored. We used the current measurements to normalize the spectra. The spectral distributions were independent of the magnitude of the tunneling current density over a range from 5×10^{-4} to 5 A/cm^2. Usually the tunneling current at constant bias decreased with running time throughout the useful life of the sample. The samples almost always began to draw more current with time just before they burned out. Occasionally a short current spike would appear on an otherwise monotonically decreasing background. Burned-out samples showed large blemished areas and sometimes small blemishes were formed during current spikes. In either case the blemishes affected the emitted spectrum. We have analyzed no data from samples that were found to have a blemish visible under a 10× power microscope after the data were collected.

The variation of the quantum efficiency between nominally identical samples was surprisingly large, as can be seen by examining Figs. 2 and 12. Factor-of-2 differences were common, and occasionally two nominally identical samples varied by as much as a factor of 10. Of these differences, only ±10% can be attributed to differences in the alignment of the sample with the spectrometer. In view of these differences between nominally identical

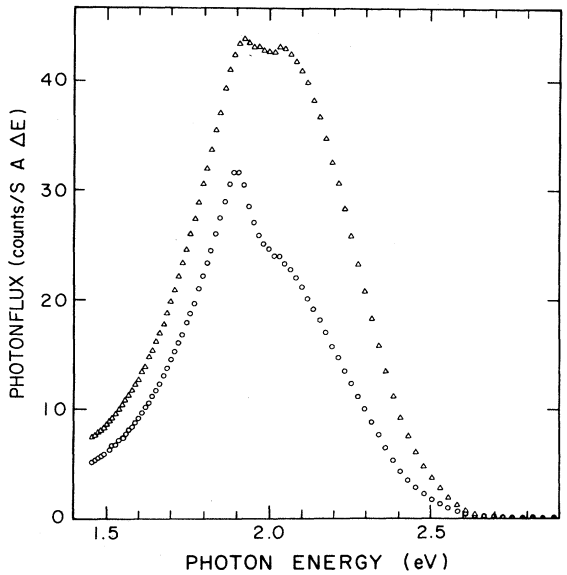

FIG. 2. Emitted spectra from the Au side of two nominally identical 30-nm Au, 38-nm al junctions. The two peaks and break in slope are universal features of Au-Al junctions. The figure illustrates the sample-to-sample variation in the spectra.

samples, one must consider samples with different film thicknesses having intensities that vary by as much as a factor of 2 or 3 to have the same quantum efficiency. We imagine that part of the difference in the efficiency is due to differences in the random roughness and dielectric functions of the sample. Some of it is also due to a decrease of the efficiency of the samples with running time that will be described in Sec. III.

Figures 2 and 12 also illustrate two universal features of our spectra. They all look as though they are composed of two peaks, one near 1.9 eV and one near 2.1 eV. In addition to the variation in the quantum efficiency, different nominally identical samples emit spectra with different weightings of the two peaks. In samples in which the low-energy peak dominates, there is always a larger break in slope in the spectra near 2.4 eV than there is in the spectra of samples in which the high-energy peak dominates. This is particularly apparent in Fig. 12.

III. EXPERIMENTAL RESULTS

Figures 3–5 show the bias-voltage dependence of the spectrum on the Au-film side. All three figures show data from the same 30-nm Au, 18-nm Al junction. Figure 3 shows the corrected spectra as a function of bias voltage. The spectra cut off near the bias voltage. The inelastic tunneling mechanism predicts a linear cutoff in the emitted intensity at the bias voltage, $P_{\text{out}} \propto (1-\hbar\omega/eV)$, at $T=0$ K if the energy dependence of the tunneling probability and voltage dependence of the barrier shape are ignored.[4] Here, $\hbar\omega$ is the photon energy and V is the bias voltage. At higher temperatures a simple calculation shows that the thermal width of the Fermi distribution smears the cutoff by about $5k_BT$. This is the same smear-

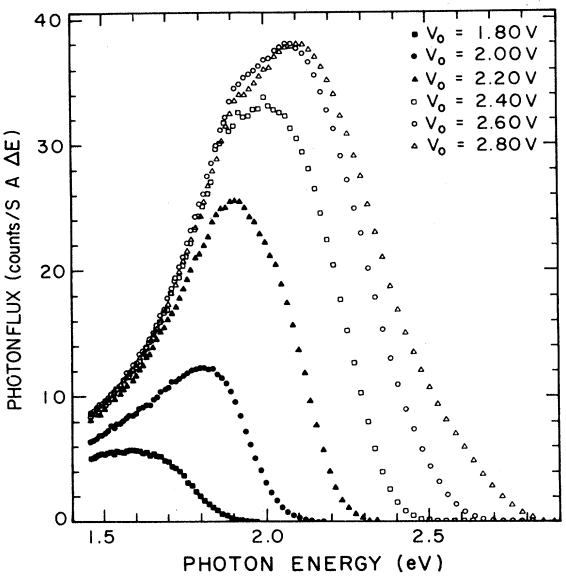

FIG. 3. Bias-voltage dependence of the Au-side emitted spectra of a 30-nm Au, 18-nm Al junction. The data show the thermally smeared cutoff at the bias voltage.

ing one obtains for linewidths in inelastic tunneling spectroscopy.[8] All of our samples were run at room temperature in air and so we must expect thermal tails of the order of 130 meV. These tails are evident in the data in Fig. 3. They are particularly easy to see for peaks biased near 2 V because they are enhanced by a peak in the emission efficiency at that energy.

In order to quantitatively investigate the adequacy of the $1-\hbar\omega/eV$ dependence, we show the spectra of Fig. 3 divided by a thermally smeared linear cutoff in Fig. 4. Similar plots were made by Kirtley *et al.* for the light

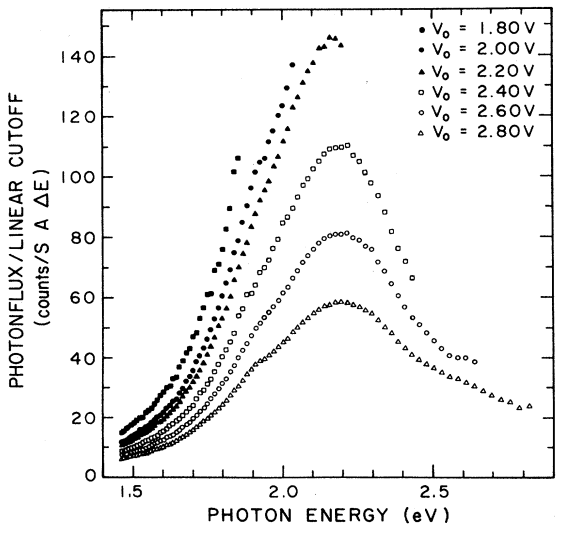

FIG. 4. Spectra of Fig. 3 divided by the thermally smeared linear cutoff function. These curves are called antenna functions.

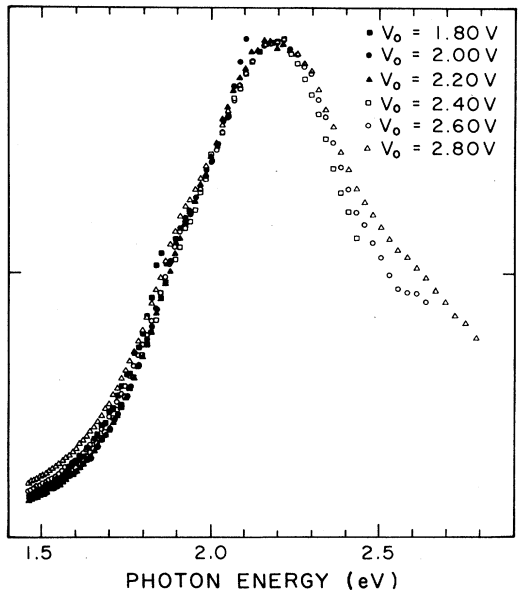

FIG. 5. Antenna functions of Fig. 4 scaled to the same peak height. The data show the similarity of the energy dependence of the measured antenna functions and illustrates the aging effect on the quantum efficiency.

emitted from Ag-Al junctions.[4,9] They called the ratio of the spectrum to the linear cutoff function an antenna factor. The Ag-Al antenna factors for different bias voltages all lie along the same monotonically increasing curve. In contrast to that, the antenna factors in Fig. 4 go through a peak near 2.2 eV and decrease in intensity with increasing bias voltage. If, however, each antenna factor is scaled by a multiplicative constant, all of them can be made to lie along the same curve. This is shown in Fig. 5.

The breadth of the thermal smearing and the similarly shaped curves that result when the spectra are divided by $1-\hbar\omega/eV$ suggest that inelastic tunneling current fluctuations are driving the modes in the film. As has been pointed out for the case of Ag-Al junctions,[4] this simple linear cutoff function works too well. When the energy dependence of the tunneling current is taken into account to generate a more realistic cutoff function, the agreement with the experiment gets marginally worse. This may be because there are several oversimplifications in the form of the fluctuation spectrum that tend to compensate one another. The need to arbitrarily scale the antenna factors to get them to lie along the same curve is new. As the junctions are run, especially at higher voltages, they deteriorate in two ways. First, they draw less current, and, second, the quantum efficiency decreases. After running the samples at 2.8 V they are less efficient as well as dimmer when the voltage is dropped to lower voltages then they were when they were first run at the lower voltages. So, whatever changes as the junction is run changes irreversibly. We do not know if impurities in the barrier introduced by our crude oxidation techniques are at fault or if the effect is intrinsic to aluminum-oxide barriers. If it is intrinsic, it makes the

practical utilization of light-emitting junctions more problematical than previously thought. The aging effect further randomizes the output of nominally identical samples because they age at different rates.

The peak in the antenna factor of Au-Al junctions is different from the monotonic behavior of Ag-Al junctions. Later on we will calculate the electric fields at various locations in the junctions as functions of $k_{\parallel}$ and $\hbar\omega$. One goal will be to identify features in the modes that contain a peak near 2.2 eV. It is this peak in the quantum efficiency that makes the thermal tails easiest to see near the biases of 2.0 V. The data in Figs. 3–5 offer some evidence that inelastic tunneling current fluctuations are at work in the junction. They also demonstrate a new, unwanted mechanism that causes nominally identical samples to behave differently.

We shall now try to determine the contribution of each mode to the light emitted from the junction. Figures 6 and 7 present evidence that the Au fast mode has little to do with the light emitted into the glass substrate from the Al film. Figure 6 shows the corrected spectra emitted from the Al-film side of three functions. All three are biased at 2.6 V and have Al-film thicknesses of 38 nm. The junctions differ in the Au-film thicknesses which are 18, 30, and 130 nm. When examined with the eye the 18-nm-thick Au sample is relatively transparent and the 130-nm-thick Au sample is opaque. This suggests that these thicknesses span a broad enough range to vary the electromagnetic energy that penetrates from the Au-air interface to the Al-substrate interface by a considerable amount. This qualitative conclusion can be quantitatively verified.[10] In spite of this range of penetration efficiency, the data in Fig. 6 show that the spectra emitted from the Al side vary by only a factor of 2 in intensity. As discussed previously, a variation of a factor of 2 is common among nominally identical junctions. Also, the intensity does not decrease monotonically with the Au film thickness. Within the variations, one must expect the emission intensities of these three samples to be identical. In Fig. 7 the data of Fig. 6 have been rescaled along the intensity axis to emphasize the similarity of the energy dependence of the three spectra. These data suggest that little of the light emitted from the Al side of the sample originates in the fields of the Au fast mode.

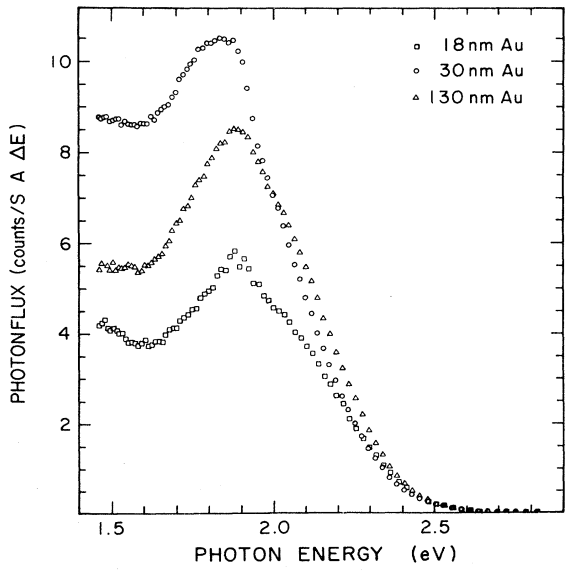

FIG. 6. Spectra from the aluminum side of three different junctions biased at 2.4 V. The Al-film thickness is 38 nm on all three samples and the Au thicknesses are 18, 30, and 130 nm. The intensities are identical within the typical scatter.

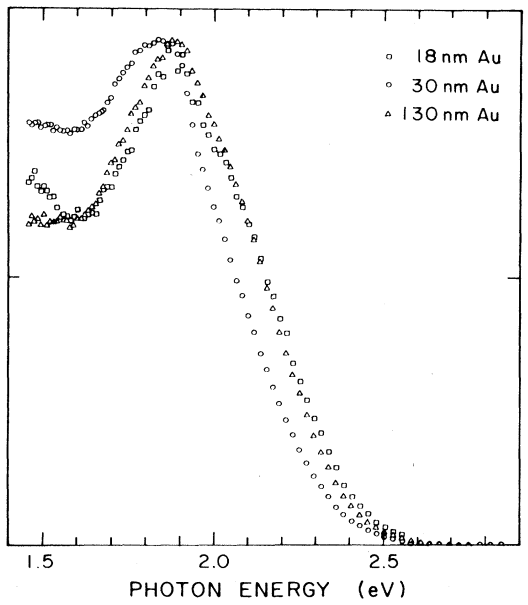

FIG. 7. Spectra of Fig. 6 rescaled to emphasize the similarity of the energy dependence of the spectra. Figures 6 and 7 show that the Au fast mode does not contribute to the emission from the Al side.

An analogous experiment can be done to assess the contribution of the Al fast mode to the light radiated from the Au side of the film. Figures 8 and 9 show the results. Figure 8 shows the emission spectra from the Au surface of three different samples. All three have 30-nm-thick Au films and are biased at 2.6 V. The Al-film thicknesses are 38, 75, and 130 nm. Again, the intensities vary by only a factor of 2 and are not monotonic in the Al film thickness. Figure 9 shows the same spectra rescaled in intensity. In both intensity and spectral shape these samples vary no more than do nominally identical samples. The conclusion is that the Al fast mode makes no substantial contribution to the light emitted from the Au surface.

So far the evidence suggests that neither fast mode contributes significantly to the light emitted from the side opposite to it. We next present the results of an experiment that suggests that the presence of the Au fast mode has little effect on the power emitted from the Au surface.

In order for a surface-plasmon polariton to exist on the interface between two semi-infinite media, the products and sums of the real parts of the dielectric functions of the two media must be negative.[11] The interface between

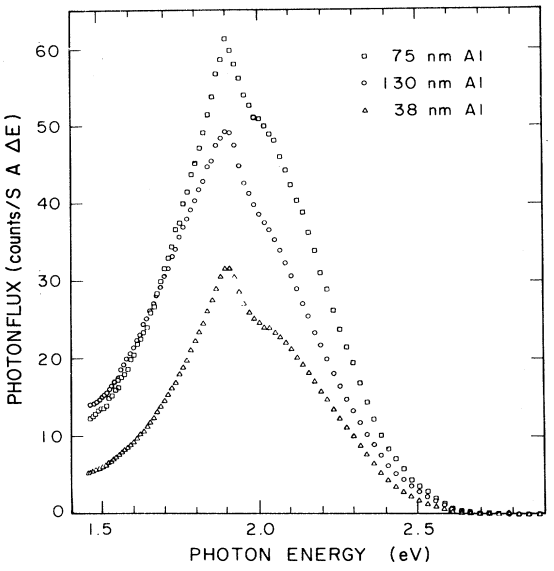

FIG. 8. Spectra from the gold side of three different junctions biased at 2.6 V. The Au film is 30 nm thick on all three samples and the Al thicknesses are 38, 75, and 130 nm. The intensities are identical within the typical scatter.

semi-infinite slabs of Au and amorphous germanium will not support a mode, because the real part of the dielectric function of *a*-Ge is more positive than the real part of the dielectric function of Au is negative throughout the visible frequency range. This suggests that a relatively thin layer of *a*-Ge deposited on the Au surface of a tunnel junction might effectively quench the Au fast mode.

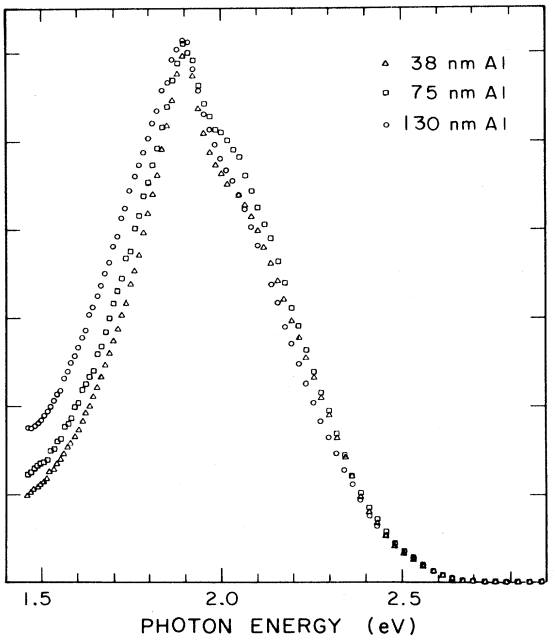

FIG. 9. Spectra of Fig. 8 rescaled to emphasize the similarity of the energy dependences of the spectra. Figures 8 and 9 show that the Al fast mode does not contribute to the emission from the Au side.

The Au fast mode on tunnel junctions can be studied using attenuated-total-reflection (ATR) spectroscopy.[12,13] In these measurements a junction is deposited on the surface of a dielectric prism. Collimated light is shined through the prism onto the Al side of the junction. Because the phase velocity of the incident light in the prism is slower than the velocity of light by a factor of the index of refraction of the prism and the Au fast mode is just marginally slower than the speed of light, light incident through the prism can be phase matched to the fast mode if the angle of incident is slightly larger than the total internal reflection angle. If, in addition, the junction is thin enough so that the incident fields reach the Au-air interface, the mode can be excited. The fields at the surface and throughout most of the structure will go through a maximum as the incident light rotates through the phase-matching angle. Two things happen at the phase-matching angle. First, because the fields become large, the dissipation in the metal films goes through a peak and the reflected power goes through a minimum. Second, because roughness at the Au-air interface can scatter the field intensity into visible light, the intensity of the scattered light will go through a peak.[14]

Figure 10 shows the results of ATR measurements on a 20-nm Au, 20-nm Al junction deposited on a hemicylindrical BK7 glass prism. The incident wavelength is 632.8 nm, corresponding to an energy of 1.99 eV. This energy is near the efficiency peak seen in the emission spectra. Curve 1 is the measured reflected intensity from

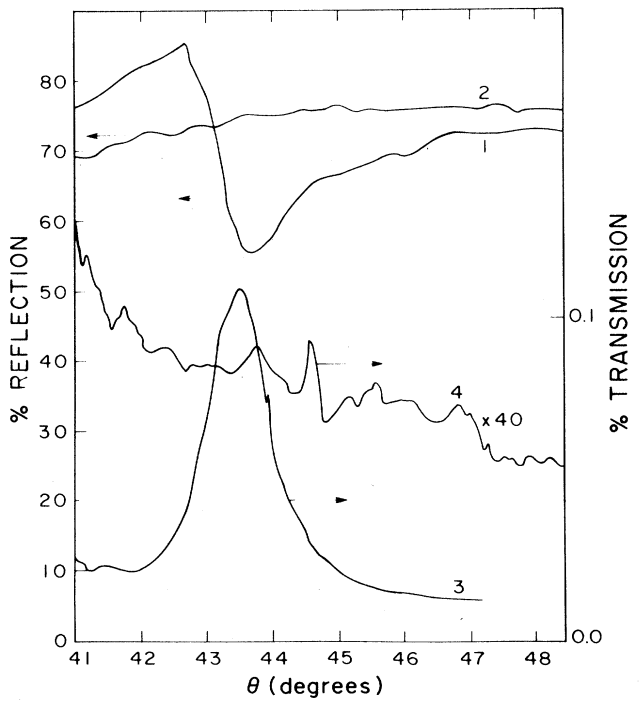

FIG. 10. ATR studies of a 20-nm Au, 20-nm Al junction, with and without a 10-nm *a*-Ge overlayer. Curve 1 is the reflection coefficient and curve 3 is the transmission coefficient of the bare junction. Curves 2 and 4 are the same coefficients for the overlayed junction. The data show that 10 nm of *a*-Ge quenches the Au fast mode.

the junction. It shows the scattered intensity measured above the Au film. It also shows minimum expected when the Au fast mode is excited. Curve 3 is the scattered intensity measured above the Au film. It also shows the behavior expected when the fast mode is excited. When this sample was made, half of it was overlaid with 10 nm of *a*-Ge. When these measurements are repeated on that part of the sample, curves 2 and 4 resulted. There is no evidence for a minimum in the reflection of the film near the Au fast mode, nor does a broader scan reveal a minimum out to incident angles of 80°. A more sensitive search for the Au fast mode can be made by looking at the scattered light above the Au film because the small intensity away from the phase-matching angle allows the gain to be increased. The gain used in measuring curve 4 is 40 times larger than the gain used in measuring curve 3. The transmitted intensity is less than 3% of the height of the peak transmission of the bare sample. The small peaks seen on curve 4 are nonreproducible noise. As anticipated, *a*-Ge overlay has destroyed or at least severely modified the Au fast mode at 1.99 eV.

Figure 11 shows the emission spectra from the Au side of a 30-nm Au, 1300-nm Al junction before and after it is overlaid with 10 nm of *a*-Ge. Although it precluded ATR measurements, we used a thick Al film in this experiment to prevent any energy from the Al fast mode reaching the Au surface. The junction is biased at 2.4 V in both cases. The intensities and the spectral shapes are identical within the usual limits. The condition of the Au fast mode is irrelevant to the emitted spectrum. This eliminates the Au and Al fast modes as sources of the light from the Au surface. The slow mode must be responsible for most of the light radiated from the Au surface of the junction.

We did not measure the spectra emitted from the Al side of junctions underlayed with *a*-Ge. Such junctions would represent a complicated case because the large negative real part of the Al dielectric function allows a mode to exist at the interface between semi-infinite Al and *a*-Ge layers. Also, because the Al fast mode lies to the right of the speed-of-light dispersion in the prism, it is inaccessible to the kind of straightforward ATR measurements we used on the Au fast mode. Such measurements would require that yet another layer be incorporated in the structure.[13] So our data do not yet eliminate the possibility that the Al fast mode contributes to the emission from the Al side of the junction. The evidence that it does not is less direct and is shown in Figs. 12–14.

Figure 12 shows the spectra of two nominally identical 30-nm Au, 38-nm Al junctions. These spectra are measured from the Au side and the bias voltage is 2.8 V. The spectra are among the most different we measured for nominally identical samples. Figure 13 shows the spectra measured from the Al side of the same two samples at the same bias voltage. Two peaks are seen on the Al side as well, and the break in slope near 2.4 eV is larger on this side than it is on the Au side. The low-energy ends of the spectra on the Al side are always more intense than the low ends of the Au-side spectra. In contrast to the color of the metals, the Al-side spectrum is redder than that of the Au side. These are universal features of the behavior of our junctions.

Figure 14 shows the ratio of the Al-side spectrum to the Au-side spectrum for each tunnel junction. The ratios have identical energy dependences and lie within 50% of each other in magnitude. All traces of both

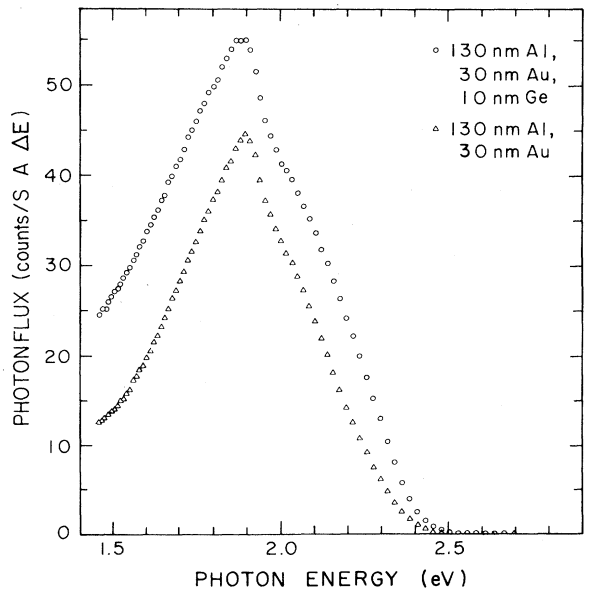

FIG. 11. Au-side emission spectra of a 30-nm Au, 130-nm Al junction with and without a 10-nm *a*-Ge overlayer. The junction is biased at 2.4 V in both cases. Along with Fig. 10, this shows that condition of the Au fast mode is irrelevant to the spectra emitted from the Au side.

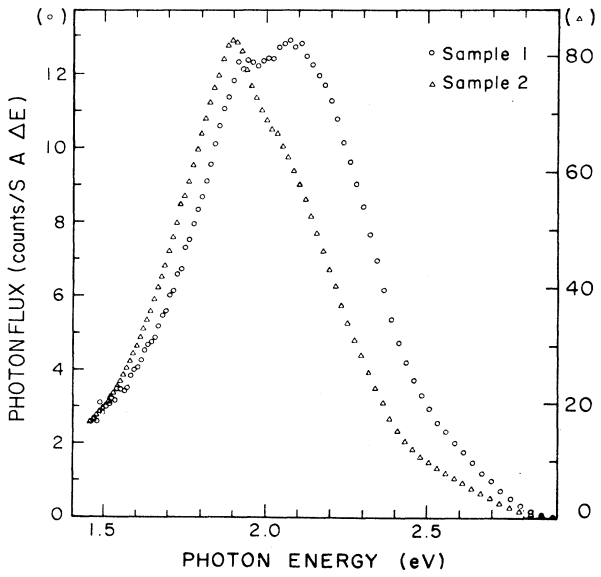

FIG. 12. Au-side emission spectra of two nominally identical 30-nm Au, 38-nm Al junctions biased at 2.8 V. In intensity and energy dependence these spectra are among the most dissimilar emitted by nominally identical samples.

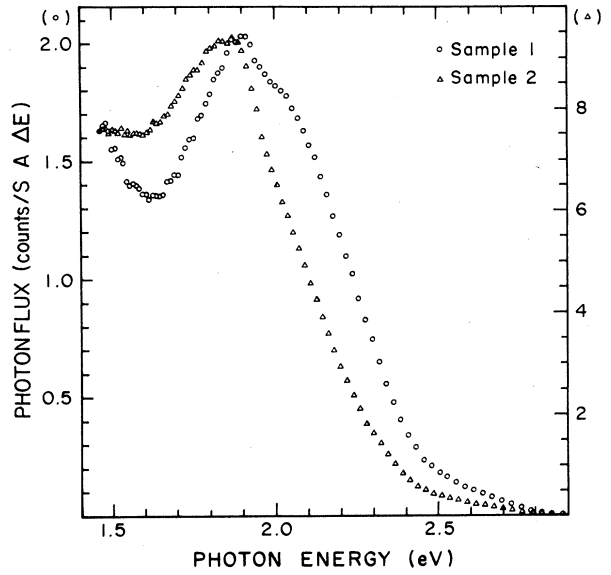

FIG. 13. Al-side emission spectra of the same junctions in Fig. 12.

peaks disappear in the ratio. We have looked at similar ratios for many samples with film thicknesses between about 20 and 75 nm for both films. Thicker films lead to dim and therefore noisy spectra off the thick-film sides and are sensitive to the dark-count subtraction. Nevertheless, in every case both peaks disappear in the ratio, and usually the size of the ratios of nominally identical samples come closer to agreeing than do the spectra themselves. This implies that the light emitted from both sides of a light-emitting tunnel junction has the same origin. The other measurements show that this origin can only be the slow mode.

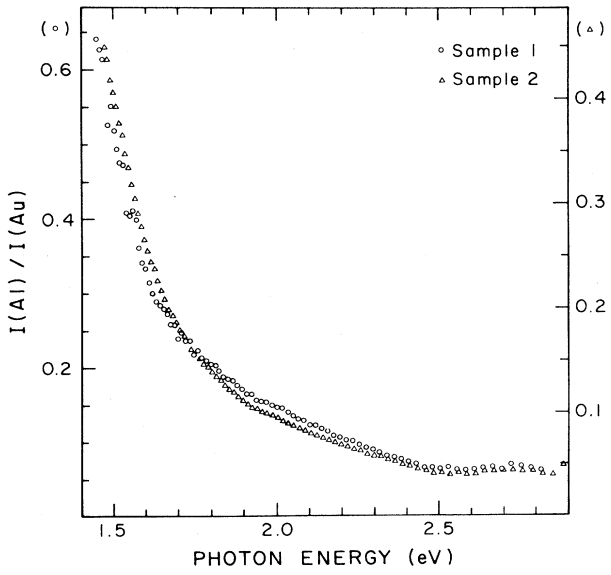

FIG. 14. Ratio of the Al-side spectra in Fig. 13 to the Au-side spectra in Fig. 12. All evidence of both peaks has disappeared and the energy dependence of the ratios is identical. The result shows that the two peaks seen off both sides have a common source.

These experiments lead to only one conclusion: the light emitted in the normal direction from both sides of small-amplitude, randomly rough Al-Au junctions is scattered from the slow-mode fields. The other two modes contribute little if anything to the emitted light.

IV. NUMERICAL RESULTS

This section describes the numerical results obtained by calculating the electric fields and the emitted spectra from tunnel junctions. When we calculate the fields we will assume that all of the interfaces are smooth and that the films are infinitely extended in the x-y plane. The purpose of calculating the fields is to try to confirm the conclusion that the slow mode is responsible for the radiation from our samples. We will also look to the field intensities as a guide in the search for the mechanism that couples the slow mode out of the junction.

After examining the fields we will calculate the power radiated from our junctions. The calculated spectra will not be quantitatively correct for two reasons. First, we will make the standard simplifying assumption about the inelastic tunneling current fluctuations.[3] Second, we are unable to calculate the intensity in any direction except strictly normal to the films. To calculate the emitted intensity, one usually calculates the fields at the interfaces of an ideally smooth junction and then allows the roughness at the real interfaces to scatter the energy in the smooth interface fields. As we will show, the field-strength contours will indicate that the emitted light is scattered from the slow mode by roughness at the edges of the oxide barriers. The presence of free charges there causes the usual formula[3] for the scattering of the z component of the smooth interface field to break down.[15] We have not yet developed the formalism to properly take the z component of these fields into account. Since the z component of the smooth interface field does not scatter normal to the junction, we can calculate the strictly normal emission without extending the formalism. This precludes an exact agreement with the measured spectra because our spectrometer accepts a rather large cone, 0.32 sr, around the normal direction. Therefore some of the measured light is scattered from the z component of the smooth interface field and is neglected in the calculation. Nevertheless, our calculated spectra will suggest the sources of all of the qualitative features mentioned in the discussion of the measured spectra in Sec. II. Also the calculated ratios of the Al-side spectrum to the Au-side spectrum will lie within a factor of 2 of the measured values over a range of samples and bias voltages for which this ratio varies by a factor of 1000. So the results of the model calculation do help clarify the emission process despite the gross simplifications made in them.

The first results we will show are calculated field strengths. We will imagine that our samples lie in the x-y plane and that the direction normal to the Au film away from the junction is the $+z$ direction. We will plot as contours above the $k_{\parallel}$-ω plane electric field strength that

results from impressing a current density

$$\mathbf{J}=J_0\hat{\mathbf{z}}\exp[i(k_{\parallel}x-\omega t)] \quad (1)$$

in the oxide barrier. The impressed current outside the barrier is zero. The field strengths shown result from setting $J_0=1.0$ statampere/cm^2. The contour plots can be thought of as the electromagnetic response function for this particular driving mechanism. We have calculated the fields by using the Green's-function technique first applied to light-emitting junctions by Laks and Mills[3] and later extended by Ushioda *et al.*[16] Because the current density we used is so simple, we checked the calculations for programming errors by recalculating the contours by matching at the interfaces fields obeying the appropriate Maxwell's equations in each layer. The results agreed. The dielectric functions used were obtained by interpolating the results tabulated by Hagemann *et al.*[17] That report shows two dielectric functions for Au. We arbitrarily used the first one. No differences that would affect our conclusions appear when the second one is used. We used 3.0 for the dielectric constant of the oxide and used the values given for BK7 glass by the manufacturer for the substrate.

Figure 15 shows the log of the absolute square of the electric field strength in the air infinitesimally above the Au film as a function of $k_{\parallel}$ and ω. The frequency range covers the entire range explored in the experiment and $k_{\parallel}$ goes out to values 6–12 times the $k_{\parallel}$ vector of free photons, depending on the frequency. We used 30, 3, and 38 nm for the Au-, oxide-, and Al-film thicknesses. These are the thicknesses used in calculating all of the field-strength contour plots shown. These are the thicknesses of the real junctions that supplied the data in Figs. 12–14. The Au fast mode is marked by what appears to be a line of peaks near the left edge of the plot. The peaks are artifacts generated when the high, narrow Au fast mode lies near a plotting grid point. The maximum square field strength occurs on the second artificial peak from the bottom. The fields of the Al fast mode are invisible on this plot, supporting the conclusion that they have little to do with the light emitted from the Au side of the junctions. The broad, low ridge in the lower right is the slow mode. Its strength at the Au-air interface is strongly attenuated by its small transverse decay length.[10]

To show the true structure of the Au fast mode, Fig. 16 shows a band of the $k_{\parallel}$-ω plane 10^4 cm^{-1} wide along the line through the maxima in Fig. 15. This region is 1% of the width of that in Fig. 15. Again, contours of the log of the absolute square of the field strength in the air infinitesimally above the Au surface are shown. We present these figures to show that neither the Au fast mode or the slow mode have a peak in their field strengths at the Au surface near 1.9 or 2.1 eV. Therefore the peaks in the measured spectra near these values are unlikely to result from the scattering of either of these modes by roughness at the Au-air interface.

Figure 17 shows the log of the absolute square of the electric field strength in the glass substrate infinitesimally below the Al film for the same 30-nm Au, 3-nm oxide, 38-nm Al junction we have been discussing. Again the field is the response to the drive term in Eq. (1) with $J_0=1$ statampere/cm^2. The $k_{\parallel}$ and ω scales are the same as in Fig. 15. The leftmost row of closed contours are the

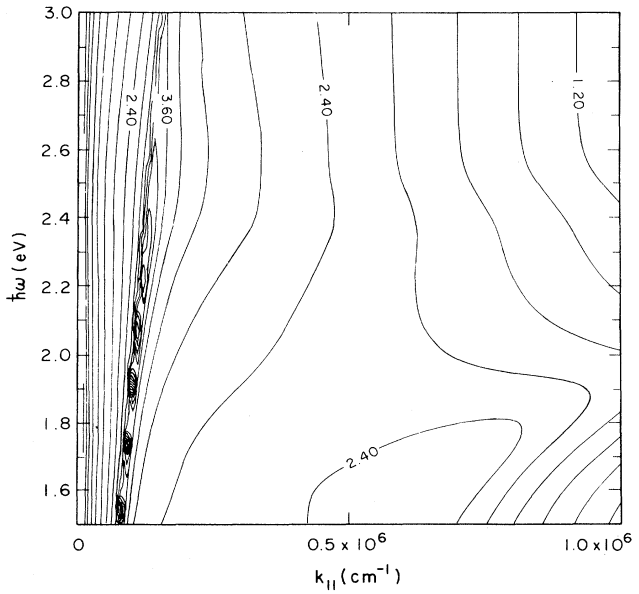

FIG. 15. Contour plot on the $k_{\parallel}$-ω plane of log of the absolute square of the E-field intensity infinitesimally above the free Au surface. The fields result from the current density of Eq. (1). The maximum value is 3.4×10^{-15} statvolts^2/cm^2. Subtract 5.4 from the number on a contour, raise 10 to that power, and multiply by the maximum value to get the square-field strength on a contour. The space is 0.3.

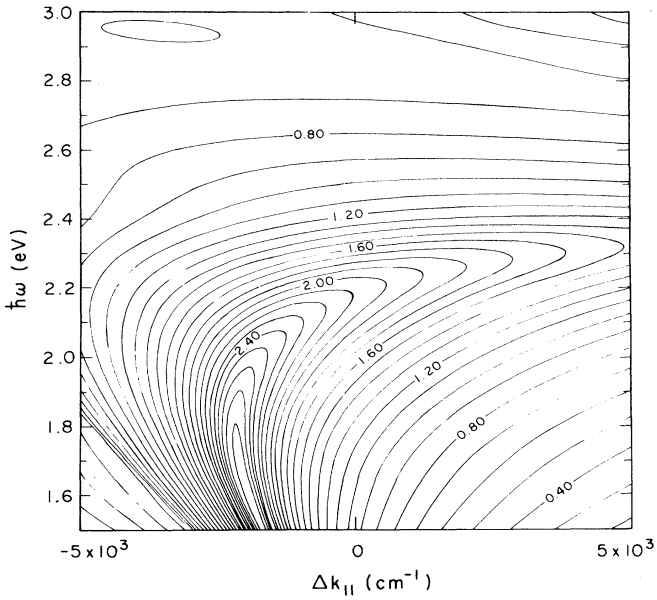

FIG. 16. Detail of the contour plot in Fig. 15 in a narrow band around the Au fast mode. $\Delta k_{\parallel}$ is the shift in $k_{\parallel}$ from the center of the mode. The maximum absolute square field strength is 1.7×10^{-14} statvolts^2/cm^2. The values on the contour are the maximum times 10 raised to the (contour value -2.92) power. The peak in the fast-mode field near 1.6 eV cannot be responsible for the peaks in the measured spectra.

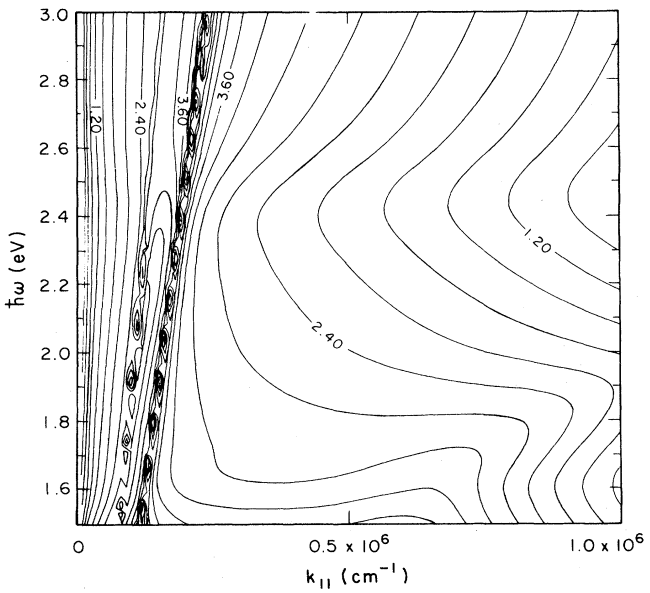

FIG. 17. Contour plot on the $k_{\parallel}$-ω plane of the log of the absolute square of the E-field intensity infinitesimally below the Al-substrate interface. The fields result from the current density of Eq. (1). The maximum value is 5.4×10^{-17} statvolts^2/cm^2. Subtract 5.79 from the value on a contour, raise 10 to that power, and multiply by the maximum value to get the mean-square field on a contour. The overall square fields here are 2 orders of magnitude smaller than the fields just above the Au-air interface.

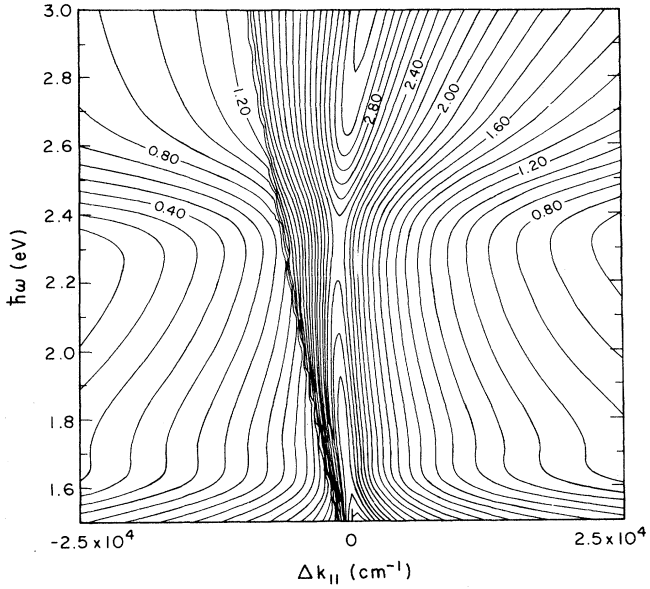

FIG. 18. Detail of the contour plot in Fig. 17 in a narrow band around the Al fast mode. The maximum square-field strength is 5.5×10^{-17} statvolts^2/cm^2. The values on a contour are the maximum times 10 raised to the (contour value -3.1) power. The Al fast mode has a saddle where the spectra have a peak and a maximum near 3.0 eV.

Au fast-mode fields that do appear at this interface in significant strength for these thicknesses. This is why the prism-coupling scheme works. The next row of closed contours is the Al fast mode. As in the case of Fig. 15, the closed contours along both modes are plotting artifacts. The maximum value occurs at the high-energy end of the Al fast mode. The fields throughout this protion of the $k_{\parallel}$-ω plane are typically 2 orders of magnitude less than those in the air at the Au interface. This is important because Fig. 14 shows that the ratio of the radiated power on the Al side to the power on the Au side is a few tenths. The slow mode is the weak ridge in the lower right corner of the plot.

Figure 18 shows the Al fast mode on a scale expanded as we did in Fig. 16. Here the width of the plot is 5×10^4 cm^{-1}, 5% of the width of the horizontal scale in Fig. 17. There is a saddle on the Al fast-mode ridge near the energy where the measured spectra require a peak to explain their emission efficiency. The maximum square field strength is at the top of the ridge.

Figures 15–18 show that the roughness in our samples would have to have an intricate and reproducible profile to scatter the field strength in any of the modes at the surfaces of the junction into the spectra we observe. An examination of the field strengths in the oxide barrier reveals a more probable source of the light.

Figure 19 shows the absolute square of the x component of the field in the oxide barrier infinitesimally close to the Au film. The energy scale is the same as in

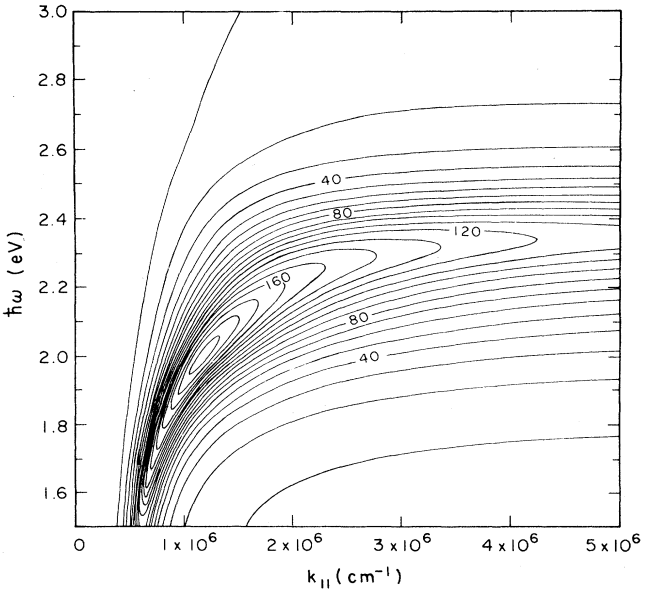

FIG. 19. Linear contour plot on the k-ω plane of the absolute square of the x component of the E field in the oxide barrier infinitesimally close to the oxide-Au interface. The maximum value is 1.9×10^{-14} statvolts^2/cm^2. The values on the contour are given by dividing the value on the contour of 195 and multiplying by the maximum value. Roughness scatters this component into the normal direction and it shows a peak near 1.9 eV. This result suggests that the slow mode is the source of the emitted light.

the previous contour plots, but the $k_{\parallel}$ range is 5 times wider. Unlike the earlier plots these are linear contours. The chief feature of Fig. 19 is the broad peak at about 2.0 eV. There is, of course, also a z component of the fields in this plane. It peaks closer to 1.6 eV. We do not show it because the z component of the field will not scatter into the normal direction to the film. The fields of both fast modes are invisible on this plot and, in fact, are invisible when the log of the absolute square field strength is plotted. Figure 19 suggests that the slow-mode field scattered by roughness at the edges of the oxide barrier might be responsible for the light emitted from our samples.

Several conclusions can be drawn from the contour plots. Neither the Au fast mode, the Al fast mode, nor the slow mode have peaks in field strength at either surface of the junction in the energy range needed to explain the peak in the measured antenna factor. Furthermore, the field strength at the Al-substrate interface is far too weak to explain the measured ratio of the Al-side to Au-side intensities unless the Al-substrate roughness is larger than the roughness at the top of the Au film. However, the parallel component of the slow mode in the barrier, the only component that scatters into the normal direction, has a peak at about the right energy. In the barrier the fast-mode fields are dwarfed by the slow-mode fields. This suggess that the slow-mode fields scattered by roughness at the edges of the barrier are responsible for the light emission.

To explore this possibility we calculated the power emitted in the normal direction by scattering off roughness at the Au-oxide and Al-oxide interfaces. The first step in calculating the power scattered by a rough interface into the normal direction is to calculate the parallel components of the fields that are present in the flat interface case as we have done in Fig. 19. Then the interface in question is allowed to assume its real profile while the **E** field is held fixed everywhere at the flat-interface value. This induces in a polarization charge density along the interface that depends on the flat-interface E_x field, the dielectric functions of the media separated by the interface, and the slope of the interface. The flat-interface fields and the induced charge density are sinusoidal in time. The two-dimensional continuity equation is then used to calculate the current density needed to conserve charge as the density oscillates in time. Finally, the current density is projected onto the flat interface, giving a current density proportional to the deviation from flatness of the real interface and a δ function. The result is

$$J_x=\frac{E_x^{(0)}}{4\pi}(\epsilon_2-\epsilon_1)\zeta(\mathbf{x}_{\parallel})\delta(z-z_i)\ , \tag{2}$$

where $E_x^{(0)}$ is the field at the flat interface, ϵ_1 and ϵ_2 are the dielectric functions on opposite sides of the interface, ζ is the deviation from flatness chosen so that $\langle\zeta(\mathbf{x}_{\parallel})\rangle=0$, and z_i is the position of the flat interface. The fields radiated by this current density add to the flat-interface fields. This approach is exactly equivalent to the perturbation-theory approximation used by Laks and Mills to generate the Green's-function solution for roughened tunnel junctions.[3]

Finally, in the absence of any experimental input, one must assume some form for the roughness profiles of the interfaces. We have made the standard assumption[3] that the power spectrum of the roughness is Gaussian,

$$|\zeta(Q_{\parallel})|^2=\pi A a^2\delta^2\exp(-\tfrac{1}{4}a^2Q_{\parallel}^2)\ . \tag{3}$$

Here, A is the junction area, a is the transverse correlation length, δ is the root-mean-square deviation from flatness, and $Q_{\parallel}$ is a wave vector parallel to films. The power scattered into the normal direction is proportional to $Q_{\parallel}$ times the power spectrum. The additional factor of $Q_{\parallel}$ is from phase space. We set the δ's and the a's equal at the two edges of the barrier and treated a as a fitting parameter. We assumed the scattering is incoherent at the two edges and added the intensities, not the scattered fields. It is possible that the surface profiles are different at the two edges, but the quantitative omissions we have made in our model do not justify the fine tuning of the calculated spectra that would result from adding more roughness parameters to the model.

Figure 20 shows a calculation of the emission spectrum divided by $1-\hbar\omega/eV$. The calculation is for a 30-nm Au, 3nm oxide, 18-nm Al junction. The transverse correlation length was varied to bring the peak to 2.2 eV. This is the position of the peak in the measured antenna factor of a junction with the same film thicknesses shown in Fig. 5. The resulting correlation length is 20 nm and we used this value in all subsequent calculations of the spectra. In the first-order treatment of the roughness, δ sets the overall magnitude of the emitted intensity, a quantity we did not measure and that did not reproduce well from sample to sample. This leaves δ undetermined. A com-

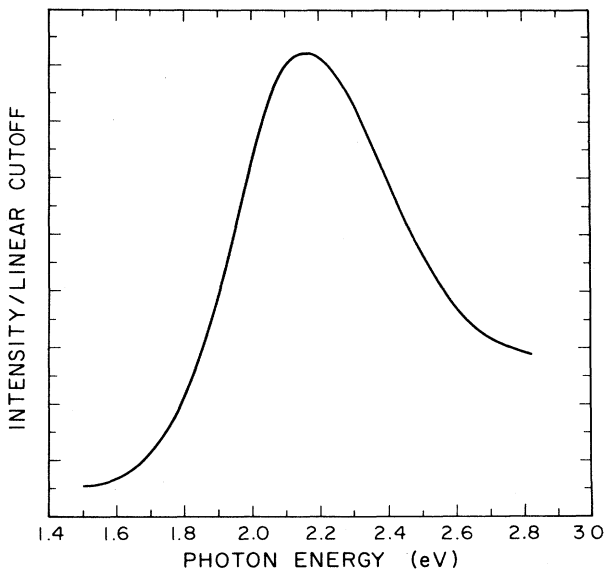

FIG. 20. Calculated spectrum divided by the linear cutoff function for a 30-nm Au, 3-nm oxide, 18-nm Al junction biased at 2.8 V. The calculation includes equal amplitude roughness with a 20-nm correlation length at both edges of the barrier. This figure can be compared with the corresponding measurement in Fig. 5.

parison between Figs. 5 and 20 shows remarkably strong qualitative agreement between the measured and calculated results. The peak in the calculated results has the same width and asymmetrical shape as the measured peak. The main deficiencies of the calculation are that there is no trace of the lower-energy peak (which is barely discernable as a shoulder in Fig. 5) and the calculation is about 20% too weak at 1.5 eV. Nevertheless, the similarity between the data and the numerical result is obvious and it strengthens the likelihood that the measured spectra result from the scattering of the slow-mode fields by the roughness at the edges of the oxide barrier.

Figures 21, 22, and 23 show the Au-side spectrum, the Al-side spectrum, and the ratio of the Al-side spectrum to the Au-side spectrum for a 30-nm Au, 3-nm oxide, 38-nm Al tunnel junction biased at 2.8 V. We assumed the same roughness parameters for this junction as for the one in Fig. 20. The results in Figs. 21, 22, and 23 can be compared with the data in Figs. 12, 13, and 14. The calculated spectra most strongly resemble the spectra emitted by sample 1 in Figs. 12 and 13. The most serious flaws in the calculated results are the complete absence of the low-energy peak and an intensity deficit on the low-energy side of the peak. Comparison of the Al-side to Au-side intensity ratios shows that both the data and the calculation have about the same energy dependence and lie within a factor of 2 of one another. This agreement is particularly striking in view of the fact that the fields on the surfaces of smooth junctions, shown in Figs. 15 and 17, are different by a factor of 100. We have varied the roughness parameters and have found that the calculated intensity ratios are less sensitive than the spectra are to the assumed roughness parameters. This may explain why the measured ratio is less sample dependent than the measured spectra, and raises the possibility that the differences between the calculated and measured spectra are due to inappropriate assumptions about the roughness parameters. We shall return to this point.

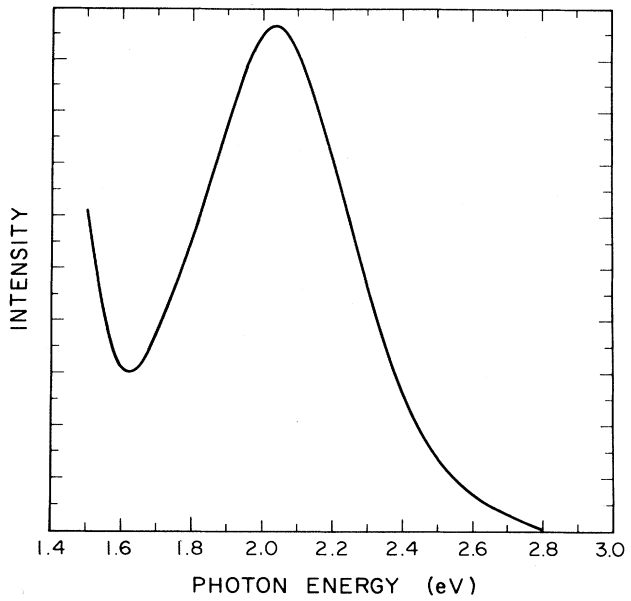

FIG. 22. Calculated Al-side spectrum for the same junction, roughness, and bias voltage as in Fig. 21. This result can be compared to the corresponding measurement in Fig. 13.

The relative sample independence of the measured ratios and the relative immunity of the calculated ratios to roughness parameters makes comparisons between measured and calculated intensity ratios worthwhile. Figure 24 shows the $\log_{10}$ of the Al-side to Au-side intensity ra-

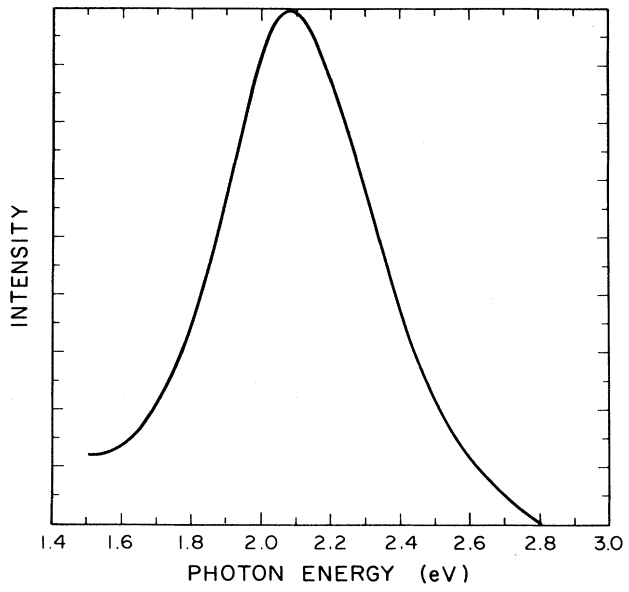

FIG. 21. Calculated Au-side spectrum for a 30-nm Au, 3-nm oxide, 38-nm Al junction biased at 2.8 V. The same roughness parameters as in Fig. 20 were used. This result can be compared to the corresponding measurement in Fig. 12.

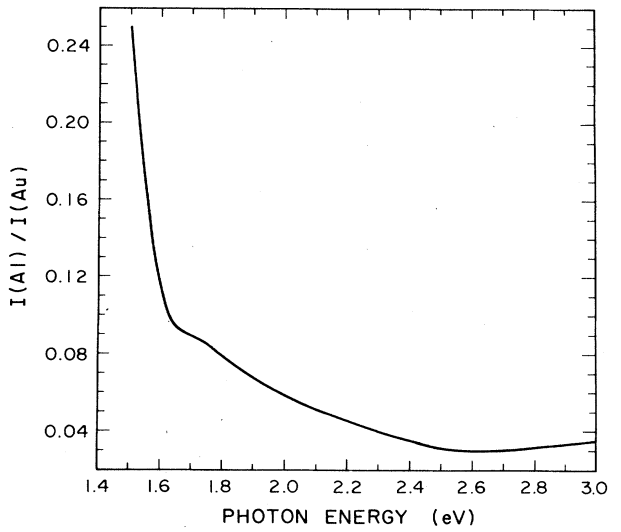

FIG. 23. Ratio of the Al-side spectrum in Fig. 22 to the Au-side spectrum in Fig. 21. The ratio has a similar energy dependence and lies within a factor of 2 of the corresponding measure ratio in Fig. 14.

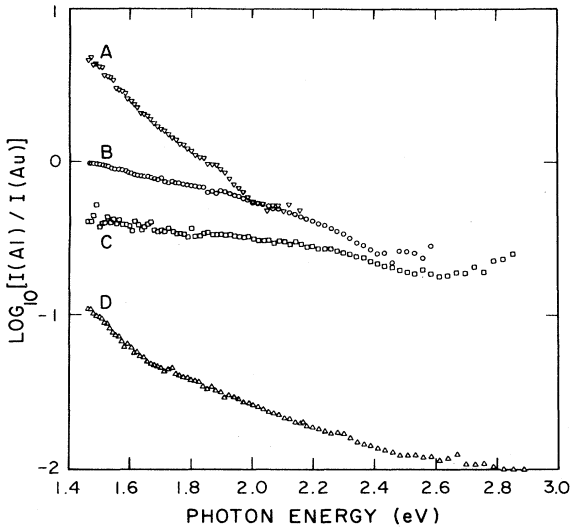

FIG. 24. Measured Al-side spectrum to Au-side spectrum ratios for four junctions. Curve A—77-nm Au, 38-nm Al; curve B—30-nm Au, 18-nm Al; curve 3—18-nm Au, 18-nm Al; curve D—18-nm Au, 38-nm Al.

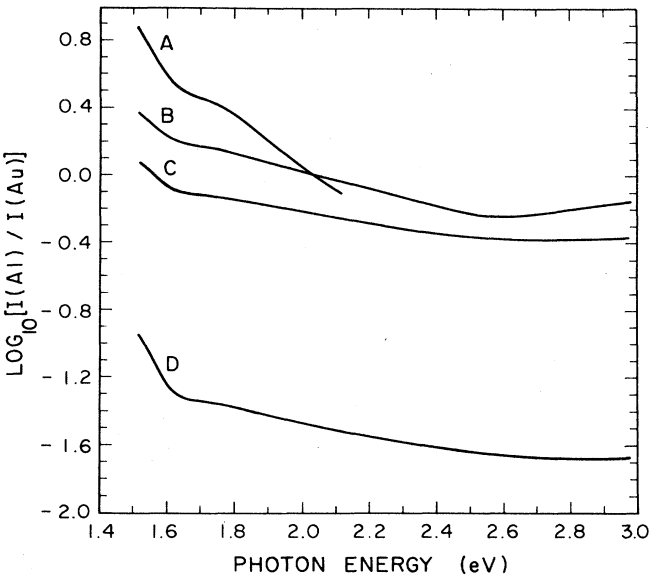

FIG. 25. Calculated Al-side spectrum to Au-side spectrum ratios for the junctions with the same film thicknesses as those in Fig. 25. We assumed 3 nm for the barrier thickness and use the usual roughness parameters. The similarity of these curves to their counterparts in Fig. 25 along with the linear cutoff are evidence for tunneling current fluctuations confined to the barrier.

tio for a range of samples. Sample A is a 77-nm Au, 38-nm Al junction; sample B is a 30-nm Au, 18-nm Al junction; sample C is an 18-nm Au, 18-nm Al sample; and sample D is an 18-nm Au, 38-nm Al junction. The ratio spans almost 3 orders of magnitude for this range of thickness and bias voltage. As usual, we looked at several samples of each type, and the scatter among nominally identical samples is about a factor of 3. Figure 25 shows intensity ratios calculated using the same roughness parameters as used to calculate the other spectra. The film thicknesses are the same as for the measured curves with the same labels and we have assumed a 3-nm oxide barrier. The calculated ratios are all about a factor of 2 smaller than the measured ratios over the entire data range. Furthermore, the energy dependence of the calculated curves is similar to the energy dependence of the measured ones. Along with the success of the linear cutoff function in reducing the measured spectra to a common curve (Fig. 5), we regard the agreement between the calculated and measured intensity ratios as strong evidence that the fields are driven by inelastic tunneling current fluctuations confined to the oxide barrier.

Finally, Fig. 26 shows a calculated emission spectrum normal to the Au film of a 38-nm Au, 3-nm oxide, 30-nm Al junction biased at 2.8 V. In this case we have made the Au-oxide interface smooth and allowed Gaussian roughness with a 20-nm correlation length to exist only at the Al-oxide interface. The result is a spectrum that looks more like sample 2 in Fig. 12 than the previous calculated spectrum does. The peak in Fig. 26 is not as sharp as the peak in the data and it has not moved all the way down to 1.9 eV. But the peak is at lower energy and it is accompanied by a more pronounced break in the slope at 2.4 eV than seen in the spectrum in Fig. 21. This suggests that the low-energy peak results from scattering at the Al-oxide interface and the high-energy peak from

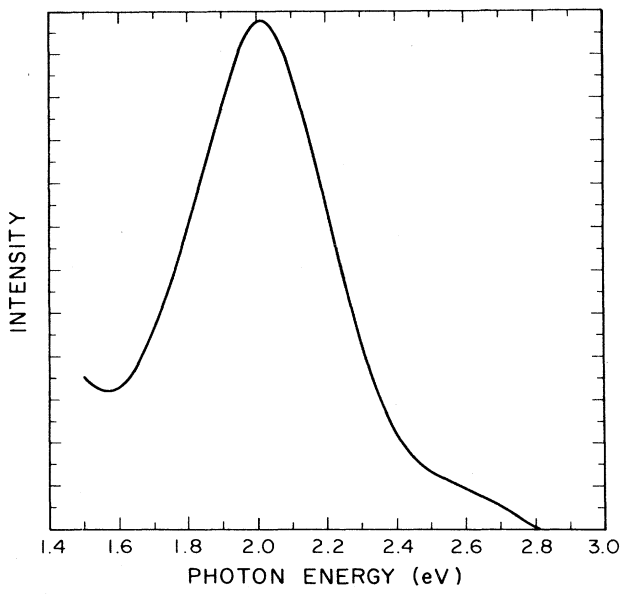

FIG. 26. Calculated spectrum off the Au side for a 30-nm Au, 3-nm oxide, 38-nm Al junction biased at 2.8 V. We assumed the Au-oxide interface is smooth, and note roughness with a 20-nm correlation length on the Al-oxide interface only. Although the peak is 0.1 eV too high, this spectrum more strongly resembles that of sample 2 in Fig. 12.

roughness at the opposite edge of the barrier. The differences in the relative amounts of each peak seen in nominally identical samples would then be attributed to differences in the roughness at these two interfaces.

V. DISCUSSION

We believe that the experiments in Sec. II show that it is the slow mode that is responsible for all but a negligible amount of the light radiated from intrinsically rough Au-oxide–Al junctions. This conclusion is reached without appeal to any model or calculation, except for the qualitative picture of the field distributions in the modes. The calculations we performed rule out either fast mode as the dominant mode because the fast-mode fields do not have peaks near 2.2 eV. The calcuations also point to the slow mode, and, in particular, the field component parallel to the plane of the sample, as the source of the light. Finally, the calculations, assuming inelastic tunnel current fluctuations confined to the barrier and including roughness only at the edges of the oxide barrier, result in reasonable spectra and ratios of spectra. These facts are evidence that inelastic tunneling current fluctuations drive the slow mode in our samples. Our conclusions are the same as those in the original paper of Lambe and McCarthy.

It is absolutely clear that the Au fast mode also radiates. There are two different kinds of experiments that unambiguously demonstrate this fact: experiments with junctions formed on gratings[9,18] and experiments with junctions formed on prism couplers.[6] In both kinds of experiments the geometry is designed to detect light phase matched to the fast-mode fields, but even in these cases we believe most of the light radiated from the junction is not from the fast mode. In both kinds of experiments on a plot of intensity *versus* angle, light emitted from the fast mode is a narrow peak on a broad background and the integrated intensity the background exceeds the intensity in the fast-mode peak. The background in those experiments is presumably the light studied here. It does not follow from the fact that fast-mode radiation can be seen in experiments designed to look for it that the bulk of the light from randomly rough junctions is scattered from the fast mode.

Other arguments have been made for the fast mode dominating the emission from randomly rough junctions.[19] The first is based on the idea that the slow-mode dispersion "cuts off" at 2.2 eV. Since Al-Au junctions show considerable intensity above 2.2 eV, it has been suggested that the cut-off slow mode cannot be responsible for the radiated light. It is true that the slow-mode dispersion curve approaches 2.2 eV asymptotically from lower energy, but, as Fig. 19 shows, the field strength in the slow mode is not a narrow ridge along the dispersion curve. The slow-mode field strength covers most of the near-infrared and visible energy range. Thus the slow-mode cutoff does not eliminate the slow mode as the source of the light.

Another argument in favor of the fast mode as the source of light is the observation that the break in slope near 2.4 eV in the spectra of many samples occurs at the same energy that the mean free path of the Au fast-mode surface-plasmon polariton abruptly decreases due to the onset of interband transitions.[19] This argument is probably false. If l_a is the mean free path for absorption and l_s is the mean free path for scattering into light for a fast-mode SPP, the probability that a SPP radiates before it decays is

$$P_R = \frac{1}{1+l_s/l_a} \ . \tag{4}$$

The data in Fig. 10 show that at 632.8 nm only 0.2% or so of the energy absorbed by the Au fast mode of a junction is reradiated. So, according to Eq. (4) we are well into the limit where the probability of emitting a photon is proportional to the mean free path for absorption. The mean free paths calculated in Ref. 19 show that l_a is a factor of 20 or so smaller at 2.5 eV than it is at 1.9 eV, the frequency of the experiment. But Fig. 5 shows that the emitted photon flux divided by the strength of the driving current is about equal at those two energies. To prevent the abrupt decrease in l_a from dropping the intensity a factor of 20, the roughness scattering must be about a factor of 20 larger for Au fast-mode fields at 2.5 eV than it is at 1.9 eV if the Au fast-mode absorption mean free path has anything to do with the emitted intensity. This is not impossible, but the relevant roughness-profile Fourier wavelengths are only 25% different at those two energies. It seems unlikely that the roughness changes so abruptly and reproducibly from sample to sample. It has also been argued that the frequency dependence of the fast mode does not identify the Au fast mode as the source of the light because the energy dependence of the slow-mode absorption mean free path is nearly identical to the Au fast-mode mean-free-path energy dependence.[20] This argument ignores the fact that the mean free path of the slow mode is less than its wavelength at energies above 2.35 eV,[10] so the mode has in some sense ceased to exist. This raises an interesting point. The calculations of the SPP mean free paths give information about the propagation of fields along the junction in a region of space free of external charge and current densities. The direct relevance of these solutions to the light-emission process is not clear to us. It seems safer to define the modes and base predictions about them on the field-response functions like those in the contour plots than it is to use the roots of the SPP dispersion relations. The field-response functions correspond more directly to the physical circumstances of the experiment.

Recently, Soole and Hughes[20] have done a similar experiment to one of ours and concluded that the Au fast mode is responsible for the light radiated from randomly rough junctions. They formed a junction on a prism and measured the angular dependence of the intensity radiated into the prism as a function of angle. They did not measure energy spectra but integrated the total intensity weighted by the quantum efficiency of their photomultiplier tube. They made a 20-nm Au, 21-nm Al junction and measured the angular dependence of the light. They next deposited an additional 20 nm of Au on the junction and repeated the measurement. Then they repeated the procedure once more. The intensity-versus-angle spectra

produced this way contained a broad background and a peak at the angle where the Au fast mode is phase matched to fields in the prism. Going from 20 nm of Au to 60 nm of Au, they observed about a factor-of-4 decrease in the background and about a factor-of-3 decrease in the fast-mode peak. They argue that this is evidence that the background, and therefore nearly all of the light radiated from their sample, originates in the Au fast mode. They ran their junctions in liquid N_2 at 77 K, so it is not clear to us whether or not the aging effect on the quantum efficiency that plagued our measurements affected theirs. At any rate, their sample and their bias voltage are different from ours. They biased their junction at 4.1 V and report a current of 1 mA. Using the Fowler-Nordheim equation to extrapolate our I-V curves to that high a voltage and scaling by the ratio of the junction areas yields well over 5 A for most of our samples. A 4.1-V bias exceeds the barrier height in the junction[21] and is nearly equal to the work functions of the metals.[22] Since our bias voltages are on opposite sides of an energy scale, the conduction mechanism across the barrier may be different from the mechanisms that predominate in thinner barriers at lower biases. Given these differences, it is not clear that our measurements and those of Soole and Hughes are as contradictory as they seem. We may be studying different devices.

Two more comments about the Au fast mode are in order. First, given the field response shown in Fig. 16, it is tempting to ascribe the intensity deficit below 2.0 eV in our calculations to the Au fast mode. It may be that if we include roughness at the Au-air interface and allow the fields to scatter there, we can improve the agreement between our calculated and measured spectra. Before we can decide if the Au fast mode is responsible for extra intensity at low energy in the measurements, we must improve our present calculation to include emission away from the strictly normal direction and perhaps include current densities in the barrier with spatial dependences that more realistically represent the overlap of the electron wave functions. Even if the Au fast mode is responsible for all of the excess measured light, only a few percent of the total number of photons emitted from our samples originates there. The Au fast mode will remain of secondary importance to the slow mode even in this case. Finally, the suggestion has been made[6] that light coupled out through the Au fast mode in prism-coupled junctions originated in the slow-mode fields and scattered into the Au fast mode through roughness somewhere in the junction. Since the wave vectors involved in scattering into the fast mode and in scattering into emitted photons are so nearly equal, one should expect both processes to occur if one does. This seems to be the case.

Arguments have been made for mechanisms other than inelastic tunneling current fluctuations driving the modes. In order to explain a factor of about 300 short fall in the calculated emitted intensity, Laks and Mills suggested that the current fluctuations must extend throughout the entire junction structure.[3] Their calculation assumed that only the Au-air interface was rough. It is likely that one can keep the current fluctuations confined to the barrier and get much larger intensities if one includes roughness at all the interfaces. From a theoretical point of view, it is desirable to keep the fluctuations confined to the barrier since they arise from the overlap of electron wave functions of different energies and the overlap is large only in the barrier. Allowing scattering at roughness at the barrier edges dramatically increases the emitted intensity for two reasons. First, the slow-mode fields are large there. Second, the slow-mode fields on smooth junctions are weak at the Au-air and Al-substrate interfaces because they are strongly attenuated in the metal films. In the case of the slow mode, the attenuation is due more to the large value of $k_{\|}$ than it is to the dielectric functions of the metals. The z component of the wave vector of a mode in a film is given by

$$k_z = \left[\epsilon \frac{\omega^2}{c^2} - k_{\|}^2 \right]^{1/2} , \tag{5}$$

where ϵ is the dielectric function of the film in question and ω and $k_{\|}$ are the frequency and wave vector parallel to the films. Because for the slow mode $k_{\|}^2$ is a large number compared to $|\mathrm{Re}(\epsilon)|$, it is mainly responsible for the large imaginary part of k_z that gives rise to the attenuation. If the roughness at the barrier shifts $k_{\|}$ to the small values between zero and the light line, the slow-mode power propagates through the film with much less attenuation.

Kirtley and co-workers[4] have argued very convincingly for a "hot-electron" drive mechanism. The data in support of this consist of measurements of the top-metal (Ag in his case) fast-mode emission peak as the morphology, thickness, and temperature of the junction are varied. Their point is that these things only strongly affect the electron mean free path in the metal and not the optical properties of the metals. Since the hot-electron mean free path affects the emitted intensity, the hot electrons must drive the mode. They also present measurements of the Ag fast-mode peak radiation in junctions driven by lasers and in charge-injection devices that have no tunnel barrier. It must be noted that the conclusion one can draw from this work is that the Ag fast mode is driven by hot electrons. This does not contradict our conclusion that inelastic current fluctuations provide nearly all the power emitted from randomly rough junctions because the slow mode, not the top-metal fast mode, dominates the emission from them.

ACKNOWLEDGMENTS

We thank Professor Gary Chanan for allowing us the use of his VAXstation for our calculations and Dr. G. Giergiel for crucial help with our computer-controlled spectrometer. This work was supported by the U.S. Army Research Office under Contract No. DAAL03-86-K-DO84.

*Present address: Department of Physics, Harvey Mudd College, Claremont, CA 91711.

[1]J. Lambe and S. L. McCarthy, Phys. Rev. Lett. **37**, 923 (1976).

[2]A useful set of references for work done before 1984 appears in P. Dawson, D. G. Walmsley, H. A. Quinn, and A. J. L. Ferguson, Phys. Rev. B **30**, 3164 (1984). More recent developments are referenced in K. Suzuki, J. Watanabe, A. Takeuchi, Y. Uehara, and S. Ushioda, Solid State Commun. **69**, 35 (1989).

[3]B. Laks and D. L. Mills, Phys. Rev. B **20**, 4962 (1979); **21**, 5175 (1980); **22**, 5723 (1980).

[4]J. R. Kirtley, T. N. Theis, J. C. Tsang, and D. J. Di Maria, Phys. Rev. B **27**, 4601 (1983).

[5]D. E. Aspnes, E. Kinsbron, and D. D. Bacon, Phys. Rev. B **21**, 3290 (1980).

[6]A. Takeuchi, J. Watanabe, Y. Uehara, and S. Ushioda, Phys. Rev. B **38**, 12 948 (1988).

[7]P. D. Sparks and R. M. Pierce, Am. J. Phys. **56**, 513 (1988).

[8]J. Lambe and R. C. Jaklevic, Phys. Rev. **165**, 821 (1968).

[9]John Kirtley, T. N. Theis, and J. C. Tsang, Phys. Rev. B **24**, 5650 (1981).

[10]B. N. Kurdi and D. G. Hall, Phys. Rev. B **34**, 3980 (1986).

[11]D. L. Mills, M. Weber, and B. Laks, in *Tunneling Spectroscopy: Capabilities, Applications, and New Techniques,* edited by P. K. Hansma (Plenum, New York, 1982).

[12]P. Dawson and J. R. Sambles, J. Phys. D **20**, 776 (1987).

[13]R. M. Pierce, J. E. Rutledge, and S. Ushioda, Phys. Rev. B **36**, 1803 (1987).

[14]J. Moreland, A. Adams, and P. K. Hansma, Phys. Rev. B **25**, 2297 (1982).

[15]The theory in Ref. 6 applies the formalism of Ref. 3 at all the interfaces without modification. This may be responsible for some of the quantitative differences between their calculations and their data, presented in J. Watanabe, A. Takeuchi, Y. Uehara, and S. Ushioda, Phys. Rev. B **38**, 12 959 (1988).

[16]S. Ushioda, J. E. Rutledge, and R. M. Pierce, Phys. Rev. B **34**, 6804 (1986).

[17]H. J. Hagemann, W. Gudat, and C. Kunz, DESY Report No. SR-74/7, 1974 (unpublished).

[18]N. Kroó, Zs. Szentirmay, and J. Félszerfalvi, Phys. Lett. **88A**, 90 (1982).

[19]The paper of P. Dawson *et al.* in Ref. 2.

[20]J. B. D. Soole and H. P. Hughes, Surf. Sci. **197**, 250 (1988).

[21]Jeff Drucker and P. K. Hansma, Phys. Rev. B **30**, 4348 (1984).

[22]Neil W. Ashcroft and N. David Mermin, *Solid State Physics* (Holt, Rinehart and Winston, New York, 1976), p. 364.